Metabolic evolution in response to interspecific competition in a eukaryote

Authors: Giulia Ghedini[1,2]*, Dustin J. Marshall[1]

Affiliations:

[1] Centre for Geometric Biology, School of Biological Sciences, Monash University, 3800 Clayton, VIC, Australia.

[2] Present address: Instituto Gulbenkian de Ciência, Rua Quinta Grande 6, 2780-156 Oeiras, Portugal.

* Corresponding author. Email: gghedini@igc.gulbenkian.pt

Abstract

Competition can drive rapid evolution which, in turn, alters the trajectory of ecological communities. The role of eco-evolutionary dynamics in ecological communities is increasingly well-appreciated, but a mechanistic framework for identifying the types of traits that will evolve, and their trajectories, is required. Metabolic theory makes explicit predictions about how competition should shape the evolution of metabolism and size but these predictions have gone largely untested, particularly in eukaryotes. We use experimental evolution of a eukaryotic phototroph to examine how metabolism, size, and demography coevolve under both inter- and intra-specific competition. We find that the focal species evolves a smaller body size in response to competition, reducing density-dependence and maximizing carrying capacity. Metabolic theory successfully predicted most of these adaptations, but we also find important departures from theory. Longer-term evolution (70 generations) led to Pareto improvements in both population growth rate and carrying capacity, suggesting that classic r-K trade-offs observed among species can be evaded within species. The evasion of this trade-off appeared to arise due to the rapid evolution of enhanced metabolic plasticity: lineages exposed to competition evolved more labile metabolisms that tracked resource availability more effectively than lineages that were competition-free. We predict that rapid evolution in both size and metabolism may be a ubiquitous feature of adaptation to changing resource regimes that occur *via* species invasions and environmental change.

Keywords: energy flux, community, species interactions, fitness, homeostasis, resources

Introduction

When ecological and evolutionary processes occur on similar timescales, eco-evolutionary dynamics can shape the diversity and functioning of communities [1–3]. Studies in bacteria imply that competition from whole communities alters evolutionary trajectories in ways that are fundamentally different from simpler pairwise interactions [4–7]. Whether these results extend to eukaryotic communities, where species tend to have lower population densities and longer life cycles, and thus slower rates of evolution, remains unclear [8]. Macroevolutionary patterns in eukaryotes suggest that competition for resources can drive species to evolve differential resource use (e.g. Darwin's finches) [9–11] but such escapes from competition may not always be accessible [12,13]. In most cases, predicting trait evolution in species that share similar niches remains a formidable challenge [8,14,15].

Metabolic theory should help with identifying the eco-evolutionary trajectories of key phenotypic traits. The theory proposes that metabolism should drive competition by setting *per capita* resource demands [16,17]. For example, because smaller organisms have lower absolute metabolic rates, their populations should support higher maximum population densities than those of larger organisms [18]. Similarly, because small organisms usually have higher metabolism per unit mass (assuming that metabolism scales hypo-allometrically with body size), their populations should grow faster than those of larger organisms – producing classic r-K trade-offs often observed among species [17]. Therefore, evolved changes in size and metabolism should both affect demography and capacity to compete with other species [19,20] but whether size and metabolism actually coevolve in response to interspecific competition has not been explored.

We combined experimental evolution and metabolic theory to determine how size, metabolic fluxes, and demography coevolve in response to both intra- and inter-specific competition in phytoplankton. We base our assessment on a focal species, the marine eukaryotic microalga *Dunaliella tertiolecta*, which we evolved for ~70 generations in each of three environments: i) competition-free; ii) intraspecific competition; and iii) interspecific competition (three other phytoplankton species). To manipulate the environment, we used dialysis bags that physically isolated the evolving population from its competitors while exposing it to competition for light and nutrients [6,21–23] (Fig. 1). We treated the competition-free lineages as a reference control. We batch-transferred both the focal species and the competitors weekly standardizing biovolumes between treatments (~7 generations). We assessed how the focal populations had evolved at two points: at ~35 generations and ~70 generations. At each

of these time points, we placed subsamples of all the evolved lineages of the focal species into a common environment, and left them for several generations such that any persistent phenotypic differences that remained among treatments represented evolved responses to the environments [24]. We assessed metabolism (photosynthesis, respiration, and net daily energy production), morphology (cell size and shape) and demography (growth rate, max. population density, and max. total biomass).

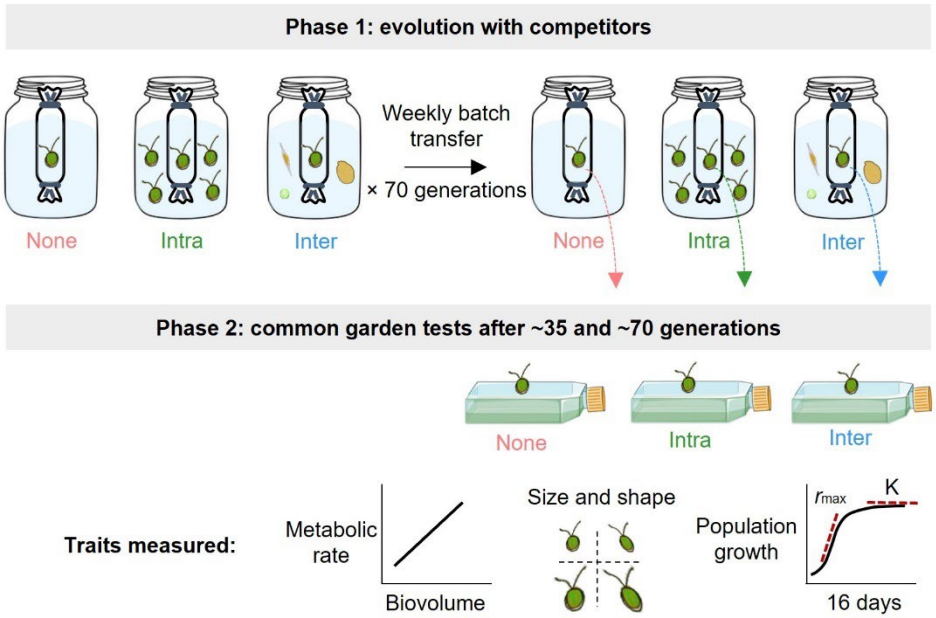

Figure 1. To test how metabolism, size and demography coevolve in response to competition, we evolved the eukaryotic microalga *Dunaliella tertiolecta* in three environments: competition-free ("none"), intraspecific ("intra") and interspecific competition ("inter"). We enclosed the focal species in dialysis bags that physically isolated the evolving population from competitors while exposing it to competition for light and nutrients for 10 weeks corresponding to ~70 generations. We propagated the focal lineages and the competitors performing weekly batch transfers. After ~35 and ~70 generations we used common garden experiments to compare changes in metabolic fluxes, morphology, and demography among the evolved focal populations.

Results

Metabolism evolves under competition

After ~35 generations of experiencing interspecific competition, algae evolved lower metabolic fluxes than algae that experienced no interspecific competition. Specifically, rates of both photosynthesis and dark respiration were lower in lineages exposed to interspecific competition (photosynthesis: competition × biovolume interaction, $F_{2,270} = 3.85$, $p = 0.02$; respiration: main competition effect, $F_{2,272} = 6.56$, $p = 0.002$; see Supplementary Information*:* Fig. S1, Table S1). These differences in metabolism were only apparent when we measured energy fluxes under resource limitation; the lineages were the same when resources were abundant (Fig. S1, Table S1). In other words, algae that experienced interspecific competition evolved plasticity to have 'thriftier' metabolisms when resources were scarce, reducing their rates of energy use, and presumably nutrient demands, while photosynthesising relative to other lineages.

After a further 35 generations of experimental evolution, interspecific competition drove more pronounced evolutionary changes in metabolism and metabolic plasticity. When we assessed metabolic fluxes under resource-limiting conditions, metabolic rates (both photosynthesis and respiration) were lowest in lineages that had experienced interspecific competition and highest in those that experienced no competition (competition effect on photosynthesis: $F_{2,47} = 6.75$, $P = 0.003$; Fig. 2b; respiration: $F_{2,47} = 15.83$, $p < 0.0001$, Fig. 2d; Table S1). Again, lineages that evolved in the presence of competition were thriftier when resources were scarce, particularly those that evolved under interspecific competition. But when we assessed metabolic fluxes when resources were abundant, the patterns were reversed: lineages exposed to competition had the highest rates of photosynthesis and respiration relative to competition-free lineages. In other words, lineages that experienced competition had evolved greater capacity to both fuel (via photosynthesis) and do (via respiration) biological work when resources were abundant (competition × biovolume effect on photosynthesis: $F_{2,210} = 3.59$, $p = 0.03$; Fig. 2a; competition effect on respiration: $F_{2,46} = 10.86$, $p = 0.0001$, Fig. 2c; Table S1). Overall then, competition-exposed lineages evolved higher levels of metabolic plasticity than competition-free lineages: competition-exposed lineages downregulated their resource demands when resources were scarce and strongly upregulated their demands during periods of resource abundance (Fig. 3). In contrast, competition-free lineages exhibited more modest metabolic plasticity in response to changes in resource availability. Together, these evolved metabolic

108 changes meant that competition-exposed lineages produced more energy on balance (photosynthesis
109 – respiration), thereby fuelling more biological work when resources were abundant (Fig. 2e), but
110 required fewer resources and produced less net energy when resource were scarce, relative to
111 competition-free lineages (Fig. 2f).

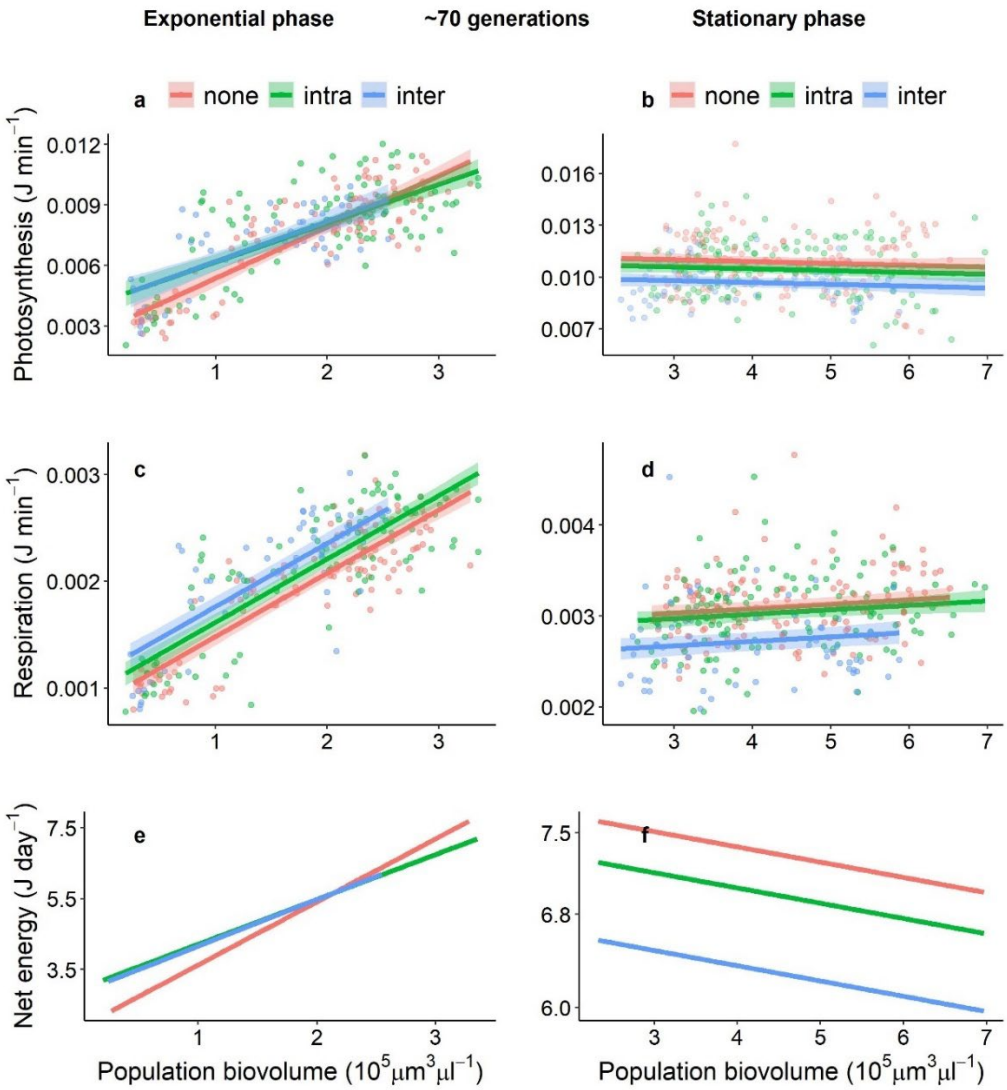

112

113 **Figure 2.** Populations exposed to interspecific competition for ~70 generations evolved greater
114 metabolic plasticity (as revealed by the relationship between population biovolume and metabolic
115 rate) than competition-free populations. Competition exposed populations had greater (a)
116 photosynthesis and (c) respiration rates when resources were abundant during the exponential
117 growth phase (left panel). But upon entering stationary phase and approaching carrying capacity
118 (right panel), populations that experienced competition from interspecifics had much lower metabolic
119 rates (b for photosynthesis, d for respiration). Integrating photosynthesis and respiration over 24
120 hours, we found that populations that had evolved in the presence of competitors produced more net
121 energy than competition-free populations when resources were abundant (e) but they also produced

122 less net energy when resources were scarce because they downregulated their metabolism relatively
123 more (f).

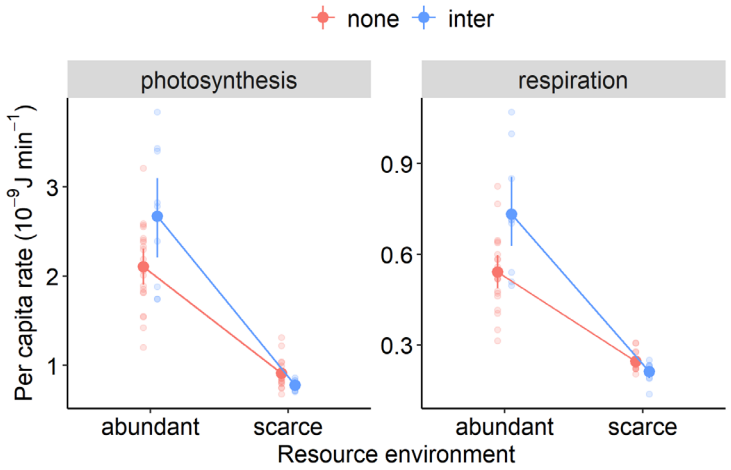

124

125 **Figure 3.** Populations exposed to interspecific competition for ~70 generations ("inter") evolved
126 greater metabolic plasticity relative to lineages that experienced no competition ("none") allowing
127 them to better track resource abundance. Cells with a history of competition increase their metabolic
128 rates (both photosynthesis and respiration) much more than control lineages when resources are
129 abundant (day 3, exponential growth phase) but downregulate them when resources are scarce (day
130 11, stationary phase).

131

132 *Size evolution, metabolic scaling and predicting demography*

133 Lineages exposed to competition evolved smaller cell sizes than lineages that were free from
134 competition (Fig. 4a for day 3 after 10 weeks; estimated marginal means for day 3: competition-free =
135 202; intra = 185; inter = 162 μm^3). After 70 generations of experimental evolution, lineages
136 experiencing interspecific competition were on average 13.4% smaller in cell volume than
137 competition-free lineages (ranging from 3.6% to 19.6% smaller during common garden experiments),
138 while those experiencing only intraspecific competition were intermediate in size (5.5% smaller on
139 average; ranging from 0.6% larger to 8.5% smaller in size than competition-free lineages)
140 (competition × time: $F_{24,564} = 3.65$, $p < 0.0001$; Fig. S2 for all days, Table S2). Cell shape coevolved
141 with cell size: lineages exposed to competitors evolved rounder cells than competition-free lineages
142 (Fig. 4b for day 3; Fig. S2; competition × time: $F_{24,564} = 8.50$, $p < 0.0001$, Table S3 for post-hoc
143 comparisons).

144 While metabolic rates often scale hypo-allometrically for eukaryotes, we found that both
145 photosynthesis and respiration rates scaled hyper-allometrically with cell size in the focal species

146 (photosynthesis: 1.31 [CI: 1.05; 1.58]; respiration: 1.28 [1.02; 1.55]; Table S4), similarly to what
147 previously found for this species [20]. But the scaling became progressively shallower as populations
148 grew denser over time (Table S4). Thus, under hyper-allometry, the smaller cells evolved under
149 interspecific competition should have lower resource demands *per capita,* in an absolute sense but
150 also relative to cell biovolume. Given the observed metabolic scalings during the exponential growth
151 phase ($B_{exponential}$ = 1.13) and stationary phase ($B_{stationary}$ = 0.60), metabolic theory would therefore
152 make the following predictions regarding the scaling of demographic parameters with cell size [19,20,25]:

153 (1) $r_{max} = M^{B}_{exponential}/M^{1} = M^{0.13}$

154 (2) $K_{cells} = M^{0}/M^{B}_{stationary} = M^{-0.60}$

155 (3) $K_{bio} = M \times K_{cells} = M \times M^{-B} = M^{0.40}$

156 From these equations, we qualitatively predict that competition exposed lineages (which evolved
157 smaller sizes) should have lower intrinsic rates of increase (r_{max}) but higher carrying capacities (K_{cells})
158 than competition-free lineages. In a quantitative sense, we also predict that growth rate and biomass
159 carrying capacity (K_{bio}) should positive covary with cell size, while population carrying capacity should
160 negatively covary with cell size (K_{cells}). We tested both sets of predictions experimentally.

161

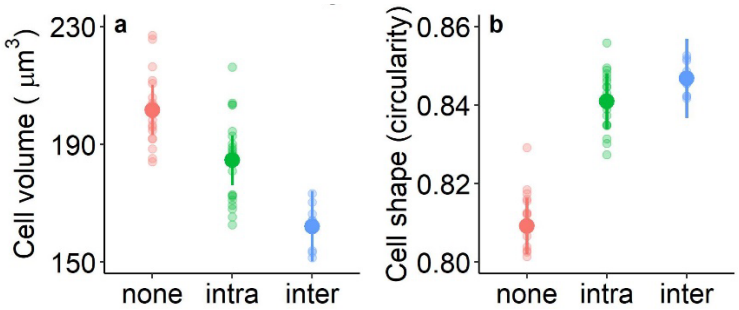

162
163 **Figure 4.** Both the size and shape of the microalga *Dunaliella tertiolecta* evolved in response to
164 competition. After ~70 generations, populations exposed to competitors evolved smaller cell sizes,
165 with a stronger decline in response to interspecific rather than intraspecific competitors (a, here
166 shown for day 3). Changes in cell size were accompanied by changes in shape: the smaller cells
167 exposed to intra- and inter-specifics competitors were also rounder than competition-free cells. See
168 Fig. S2 for the complete temporal series.

169

The evolution of greater carrying capacity

We found strong qualitative and quantitative support for our demographic predictions based on metabolic theory. After ~35 generations, lineages that experienced competition had lower maximum growth rates but greater carrying capacity (K_{cells}) than competition free lineages, displaying a classic r-K trade-off (effect of competition on r_{max}: $F_{2,42} = 10.46$, $p < 0.0005$, Fig. 5a; effect on K_{cells}: $F_{2,42} = 19.18$, $p < 0.001$, Fig. 5b). After 70 generations of experimental evolution, we found the same evolved difference in carrying capacity (K_{cells}; $F_{2,46} = 13.91$, $p < 0.001$, Fig. 5d) but the competition-exposed lineages showed maximum population growth rates that were similar to the competition-free lineages ($F_{2,46} = 1.97$, $p = 0.15$, Fig. 5c; Table S5). The evolved demographic responses were similar regardless of whether competition was intra- or inter-specific (Fig. S3, Table S5).

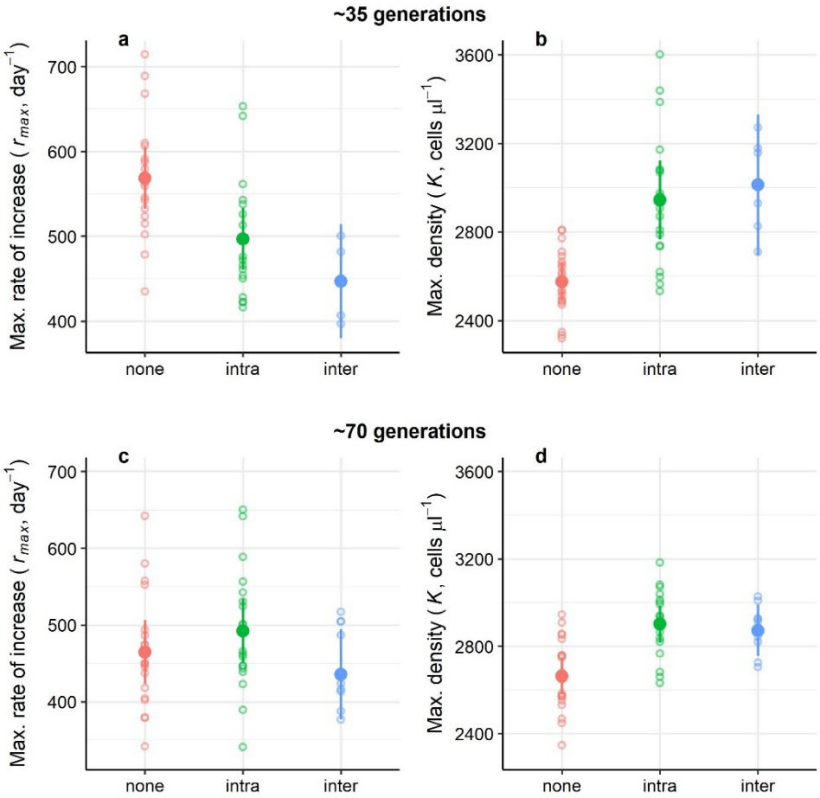

Figure 5. Populations that experienced competition had lower maximum population growth rates but greater carrying capacity in terms of cell numbers after 5 weeks of experimental evolution (~35 generations, top row). Differences in carrying capacity persisted after a further 35 generations but with no differences in growth rates between competition environments (bottom row). At either time, the type of competition experienced (intra- or inter-specific) did not affect demographic parameters.

We compared our quantitative predictions derived from metabolic theory with the observed scaling of each demographic parameter with cell size for the focal populations, and found remarkably strong congruence between the two for most parameters. We find that K_{cells} declines (c.f.: observed = –0.56; predicted = –0.60; $F_{1,48}$ = 22.4, p < 0.001; CI: –0.79; –0.32; Fig. 6b) and K_{bio} increases with size as predicted by theory (c.f.: observed = 0.44; predicted = 0.40; $F_{1,48}$ = 14.1, p < 0.001; Fig. 6c). But we find a slightly weaker than predicted relationship between r_{max} and size (c.f.: observed= 0.06; predicted = 0.13); this relationship is non-significant as the confidence intervals overlap zero ($F_{1,48}$ = 0.02, p = 0.88; CI: –0.71; 0.83; Fig. 6a).

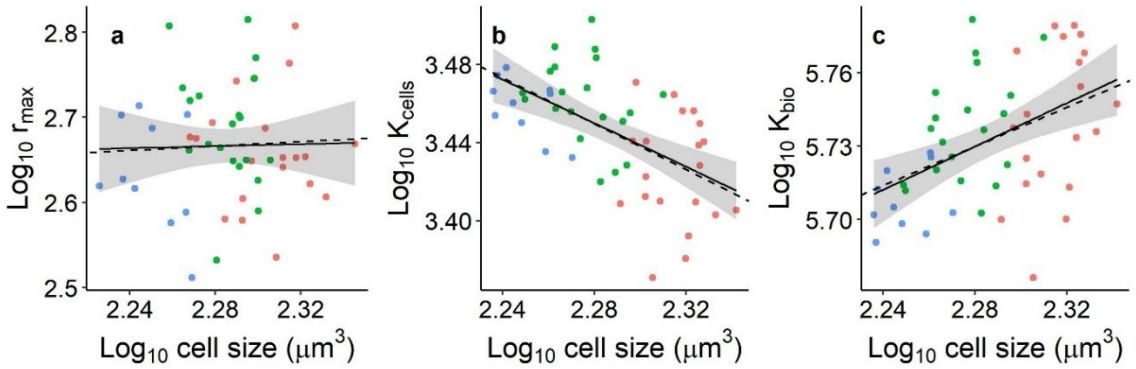

Figure 6. We find strong congruence between predictions from metabolic theory (broken lines) and demographic observations (solid lines). The scalings of max. growth rate (r_{max}), max. population density (K_{cells}) and max. biovolume (K_{bio}) with cell size observed from our data after 70 generations are: r_{max} = observed 0.06 (CI: –0.71; 0.83); predicted 0.13; K_{cells} = observed –0.56 (CI: –0.79; –0.32); predicted –0.60; K_{bio} = observed 0.44 (CI: 0.21; 0.68); predicted 0.40. Scaling exponents are calculated for the 3 competition treatments together (blue = inter; green = intra; red = competition-free). We calculated the expected scaling of r_{max} as the average scaling observed over the first 5 days because population growth is determined early on (exponential growth phase); we calculated the expected scaling of K_{cells} and K_{bio} as the average scaling over the last 3 sampling days (12 to 16) when cultures were in stationary phase and because cell size stabilised from day 12 onwards (Fig. S2). We used the same range of days to calculate the average cell size for each replicate shown above (hence differences in size on x-axis between panel a and panels b-c).

208 **Discussion**

209 We found that intra- and inter-specific competition drove the evolution of cell size and metabolism in
210 the eukaryote *Dunaliella tertiolecta* in ways that metabolic theory anticipates. Because metabolism
211 scaled hyper-allometrically with cell size in the focal lineages, the evolution of smaller sizes in
212 response to competition reduced *per capita* resource demands (both in absolute and relative terms),
213 such that cells achieved higher population densities but lower total biomass. These increases in
214 population carrying capacity initially came at the expense of population growth rates – after only 35
215 generations of experimental evolution, the focal lineages experienced the classic trade-off between
216 population growth rate and carrying capacity. However, through further evolution (~70 generations),
217 competition-exposed lineages achieved Pareto improvements in demography: their max. population
218 growth rates were comparable to those of competition-free lineages while also maintaining higher
219 carrying capacities (Fig. 5). The evolution of greater metabolic flexibility appeared to enable this
220 change; competition-exposed lineages were able to better downregulate their energy fluxes when
221 resources were scare but strongly upregulated their metabolism when resources were abundant,
222 thereby increasing both population growth rates and carrying capacity. This finding represents a novel
223 departure from theory as the evolution of enhanced metabolic plasticity was unanticipated by any
224 theory base but, in hindsight, seems almost inevitable. We eagerly await further studies that test the
225 role of competition in driving metabolic plasticity in other systems. Enhancements in plasticity might
226 explain why within-species patterns may not always reflect the same trade-offs observed among
227 species [14,26].

228 Metabolism sets resource use and fuels growth, so metabolic rate should be under selection when
229 competition is intense [27]. Classic macroevolutionary patterns suggest that competition selects for
230 efficiency which is often associated with larger body sizes and lower metabolic rates because
231 metabolism scales hypo-allometrically in most metazoans [28–30]. In contrast, our species exhibits
232 hyper-allometric scaling of both photosynthesis (1.31) and respiration (1.28) with cell size so, while
233 larger cells produce relatively more energy *per capita*, they are also both absolutely and relatively
234 more expensive to maintain. Therefore, lineages exposed to competition evolved smaller, more
235 resource-efficient cells. Interestingly, Long Term Experimental Evolution (LTEE) in *E. coli* yielded the
236 opposite evolutionary trajectory of cell size to produce the same outcome – cells became larger over

time to enhance resource-use efficiency [25]. The trajectories of cell size in both studies actually accord with metabolic theory. In both, cells change size such that size-specific metabolic rates decrease (metabolism scales hypo-allometrically with size in the LTEE). Metabolic theory also predicts the relationships between size, density, and biomass in each study (based on species-specific metabolic scaling relationships). Based on our results and those of Marshall et al. [25], we would therefore predict that competition should select for smaller body size in species which show hyper-allometric metabolic scaling, but larger body size in species that show hypo-allometric scaling. For metazoans, most species show hypo-allometric metabolic scaling within species (the appropriate biological scale in this instance), whereas intraspecific metabolic scaling in unicellular organisms remains largely unexplored except for a few cases. We look forward to future studies that explore how metabolic scaling and competition interact in other species, particularly other microbial species given their pivotal role in driving biogeochemical cycles [31,32].

Our findings have some concerning implications regarding global change. Phytoplankton play a key role in the global carbon budget, accounting for ~50% of all carbon fixed annually; thus, any change in phytoplankton productivity will strongly influence global carbon fluxes [33]. Increased water stratification due to ocean warming will intensify resource competition and decrease cell size within species [34,35]. Our competition-exposed lineages evolved smaller cells in response to stronger resource competition – in that sense, our experimental evolution mimics the impacts of global change. We found that the net energy fluxes of the competition-exposed lineages were ~15% lower in the stationary phase than those of competition-free lineages (Fig. 2f). Hence the net carbon assimilation rate of our evolved lineages was systematically lower. If natural phytoplankton populations also evolve smaller cell sizes in response to warming and/or nutrient limitation (and initial studies suggest that they do) [34], then our results would imply that rates of carbon assimilation and phytoplankton biomass will decline with further global change, creating a positive feedback loop. While thermal adaptation might dampen the negative effects of warming on phytoplankton productivity [36,37], species interactions can increase the sensitivity of species to global change through resource competition [7,38] and alter their evolutionary rates in ways that are poorly resolved [4,6]. Our results suggest that competition for resources might compound the impacts of global change by further selecting for smaller cell sizes and thriftier metabolisms that better tolerate competition but that may have undesirable impacts on carbon fixation.

Evolution happened rapidly in our system (within 70 generations). Such rapid evolution was likely fuelled by the very large population size of the founding populations (~5 million cells). These rates of evolution are comparable to those observed in other experimental evolution studies of phytoplankton where size and metabolic traits evolved within 100 generations [37,39,40], whereas it takes longer for evolution to manifest when populations are derived from a single clone [41]. Overall, competition from a community exerted stronger effects on the evolution of these traits than intraspecific competition, possibly because diverse competitors consume available resources more rapidly and effectively [42,43]. Thus, by posing a stronger selective pressure, competition from a community speeded up adaptation countering the negative effects of reduced population sizes due to stronger resource competition [44], similarly to what observed in bacteria [4,5]. Still, we find remarkable consistency between the evolutionary responses to intra- and inter-specific competition, with both selecting for smaller, more efficient cells able to sustain greater maximum population densities. Carrying capacity (or equilibrium population size, K), rather than growth rate, is thus the quantity maximised by competition as predicted by life history theory for stable or low stochastic environments [45–47]. Selection for r-K traits has been demonstrated in numerous systems within species [27,46,48] but few studies have demonstrated the same principle in response to interspecific competition. MacArthur & Wilson first hypothesized in 1967 that selection for K should also apply in a community when species compete for similar resources [45] but, to our best knowledge, these results are a first experimental demonstration that this demographic prediction of life history theory also holds under interspecific competition.

Since size and metabolism together determine resource access and use [34,49,50], changes in both traits might be a common feature of how species cope with shifts in competition and resource regimes. Both size and metabolic evolution might become more common, or rapid, as climate change, species introductions and biodiversity loss alter competition for resources [51,52]. It seems likely that metabolic evolution will underpin many human-induced changes in resource regimes as well as mortality risks [53], and we look forward to future studies that search for signatures of shifts in metabolism associated with changes in competition regimes.

294 **Materials and Methods**

295 *Overview of experimental set up*

296 We tested the effects of competition on the metabolic fluxes, morphology, and demography of the
297 eukaryotic unicellular alga *Dunaliella tertiolecta*, which we obtained from the CSIRO Australian
298 National Algae Culture Collection (ANACC, strain CS-14). To manipulate the competitive
299 environment, we enclosed the focal species in dialysis bags which were then placed in one of three
300 environments for 10 weeks (1st June to 10th August 2021, ~70 generations): 1) surrounded by media
301 with no competitors (competition-free), 2) by a population of conspecifics from the same strain
302 (intraspecific competition) or 3) by a community of three other phytoplankton species (interspecific
303 competition). For this latter treatment, the species were chosen to represent different sizes and
304 phytoplankton groups: *Amphidinium carterae* (CS-740), *Phaeodactylum tricornutum* (CS-29) and
305 *Nannochloropsis oculata* (CS-179) (Fig. 1, phase 1). Every week we batch-transferred both the focal
306 species and the competitors (~7 generations). After 5 and 10 weeks (~35 and ~70 generations,
307 respectively), we quantified changes in the traits of the focal species in common garden experiments
308 (phase 2).

309 We sourced all phytoplankton species as 20 ml populations from CSIRO algal collection, Australia.
310 We grew each population individually in 2 L glass bottles with standard f/2 enriched seawater medium
311 enriched with silica for a month prior to the experiment, transferring each population into fresh media
312 every week. The same medium was used throughout the experiment and common gardens. The
313 medium was prepared with 0.45 µm filtered seawater and autoclaved following the recipe of Guillard
314 & Ryther, 1962 [54]. All experiments were performed in a temperature controlled room (20 ± 1°C) on a
315 14:10 hours light:dark cycle and the cultures were grown under a light intensity of 115 ± 5 µmol
316 photons m^{-2} s^{-1}.

317 *Phase 1: evolution with competitors*

318 The dialysis bags in which we enclosed the focal species enabled competition for light and nutrients
319 but prevented cell mixing among phytoplankton species and exchange of bacteria (MWCO 12-14000
320 Da, pore size 24 Angstrom). Each bag contained a volume of 35 ml and was placed at the centre of a
321 500 ml glass jar assigned to one of the three competition treatments above (n = 20 for each
322 competition treatment).

323 We started the experiment with an initial biovolume of 9.6×10^8 μm^3 of the focal species which
324 corresponded 5×10^6 cells. This large inoculum size meant that the founding populations likely
325 contained a large amount of standing genetic variation. The glass jars containing the competitors
326 were filled to 350 ml to completely submerge the dialysis bag. To maintain the same biovolume to
327 media ratio, the initial biovolume of the competitors was 10 times that of the focal species (i.e. $9.6 \times$
328 10^9 μm^3). We added the three competitor species of the interspecific treatment in equal biovolumes.
329 The jars of the control treatment (competition-free) were filled with media only.

330 We quantified biovolume as the product of cell density and cell size obtained for each species from
331 two 10 µl samples, fixed with 1% Lugol's solution. For each sample, we took 20 photos equally
332 spaced around the cell-counting grid of a Neubauer counting chamber (ProSciTech, Australia) under
333 an Olympus light microscope at 400× magnification. We analysed the images with ImageJ and Fiji
334 software (version 2.0) [55] to quantify the number of cells (cells μl^{-1}) and their size (µm, length and
335 width; diameter for *Nannochloropsis*). We calculated cell volume by assigning to each species an
336 approximate geometric shape [56] (prolate spheroid $V = (pi/6) \times width^2 \times length$ for all species except
337 *Nannochloropsis* which we treated as a sphere $V = (pi/6) \times diameter^3$). Cell circularity is calculated by
338 the Fiji software as $4 \times pi \times (area/perimeter^2)$ and ranges from 0 to 1 (perfect circle).

339 Each week we transferred the same initial biovolume of the focal species and the same initial
340 biovolume of the competitors to a new, sterilized set of dialysis bag and jar. Cell densities, size and
341 biovolume were determined as described above. We did not manipulate the relative abundance of
342 species in the interspecific treatment. In weeks 3, 5 and 6 the cell densities of the focal species were
343 very low in the interspecific treatment – had we reinoculated the same initial biovolume we would not
344 have been able to add fresh medium. To avoid this nutrient limitation, we reinoculated only half of the
345 initial biovolumes across all treatments. By week 6, we discarded 13 lineages of the focal species in
346 the interspecific treatment because they were contaminated by one of the interspecific competitors
347 (the diatom *Phaeodactylum tricornutum*). To continue the experiment, we established an additional
348 lineage from each of the remaining seven replicates. By the end of the experiment, we lost 4 other
349 replicates in the interspecific treatment because of *Phaeodactylum*'s contamination.

350 The batch-transfer approach meant that all populations in our experiment experienced fluctuating
351 densities, but those surrounded by competitors always faced greater densities and thus competition.
352 Shifts in densities are common in nature and mediate the balance between density-independent and

353 density-dependent selection (r- and K-selection) [45]. If stochasticity is low, life theory predicts that
354 selection for K should prevail even under fluctuating conditions [28,47,57].

355 *Phase 2: common garden experiments*

356 We quantified evolutionary changes in the metabolism, morphology and demography of the focal
357 species in two common garden experiments; the first after five weeks of evolution with competitors
358 (~35 generations) and the second after ten weeks (~70 generations). Before each common garden,
359 we grew the focal species in a neutral environment for two generations to reduce any environmental
360 conditioning (neutral selection). Both for the neutral selection and common garden, we inoculated an
361 equal biovolume of each lineage in cell culture flasks (n = 20 for the no competition and intraspecific
362 treatments, n = 6 and n = 10 for the interspecific treatment in the first and second common garden,
363 respectively). Biovolume was determined as before from the average cell size and cell density of each
364 lineage; we decided a priori to add 15 ml of the lineage with the limiting biovolume (~14×10^8 μm^3),
365 back calculated the volumes of the other lineages and added 100 ml of media (f/2 + silica, as above)
366 to all flasks. The two common gardens started on 8th July and 12th August 2021, respectively, and
367 lasted 16 days, which was the approximate time needed for the cultures to reach carrying capacity –
368 one of the key traits we wanted to phenotype. We discontinued the common garden after 16 days to
369 avoid further evolution or adaptation by the focal lineages to the common garden conditions. Each
370 day, we removed 10 ml from each culture flask for sampling and replaced it with fresh media. In the
371 first common garden we sampled every day except on days 6, 10, 13 and 15; in the second we
372 sampled every day except on days 7, 13 and 15.

373 *Trait measurements*

374 Each sampling day, we fixed 1 ml sample with 1% Lugol's solution to quantify the cell size (volume),
375 shape (circularity) and abundance of each lineage as described above. We assessed changes in cell
376 shape in addition to size because the shape of a cell can mediate access to resources and is thus an
377 important component of fitness in unicellular organisms [34,58–61].

378 We measured oxygen evolution rates in 5 ml samples using 24-channel optical fluorescence oxygen
379 readers (PreSens Sensor Dish Reader, SDR; AS-1 Scientific Wellington, New Zealand) following
380 established protocols [62,63]. Sensors were calibrated with 0% and 100% air saturation before the
381 experiment. Net photosynthesis (oxygen production) was measured under the light intensity at which

382 the cultures were grown for 20 minutes, followed by 1 hour in the dark to measure respiration rates.
383 Thirteen blanks were filled with the media obtained from centrifuged samples (spun at 2,500 rpm for
384 10 min to separate the algae from the supernatant) to correct for background microbial activity since
385 cultures were not axenic. Prior to measurements, samples were spiked with 50 µl of sodium
386 bicarbonate stock for a final concentration of 2 mM sodium bicarbonate to avoid carbon limitation.

387 The change in percentage oxygen saturation was calculated with linear regressions using the LoLinR
388 package [64]. The rate of photosynthesis or respiration of the whole sample (VO_2; units µmol O_2/min)
389 was then measured as $VO_2 = 1 \times ((m_a - m_b)/100 \times V\beta O_2)$ following [65], where m_a is the rate of change
390 of O_2 saturation in each sample (min^{-1}), m_b is the mean O_2 saturation across all blanks (min^{-1}), V is
391 the sample volume (0.005 L) and $V\beta O_2$ is the oxygen capacity of air-saturated seawater at 20°C and
392 35 ppt salinity (225 µmol O_2/L). The first three minutes of measurements in the light were discarded
393 for all samples. Respiration rates were calculated after 15 minutes of dark when oxygen levels started
394 to show a linear decline. Photosynthesis and respiration (µmol O_2/min) were converted to calorific
395 energy (J/min) using the conversion factor of 0.512 J/µmol O_2 to estimate energy production and
396 energy consumption, respectively [66].

397 *Statistical analyses*

398 All analyses and plots were done in RStudio (version 4.1.3), separately for the two common gardens,
399 using the main packages nlme [67], lme4 [68], car [69], and ggplot2 [70].

400 Morphology. We assessed differences in cell morphology (size and shape) with linear mixed models
401 including competition treatment (3 levels) and time (day) as categorical predictors, and lineage
402 identity as random intercept to account for repeated measures; time was considered categorical
403 because the relationship with cell morphology was non-linear. We take day 3, during the exponential
404 growth phase, as a reference to report post hoc results on differences in cell size and shape in the
405 main text, and we report post hoc results for each day in supplements.

406 Metabolism. While oxygen rates increased linearly with biovolume over the first few days, this
407 relationship broke down as biovolume increased (over ~3 μm^3/µl) (Fig. S4). Log-transformation did not
408 result in linearity across the entire range of biovolume. Therefore, we analysed oxygen rates
409 separately for the first part of common gardens during the exponential growth phase (from day 1 to
410 day 6 included), and for the second part during the stationary phase (day 7 to 16). We used linear

411 mixed models with biovolume (covariate) and competition treatment as predictors, and lineage identity
412 as random intercept for the data of the second common garden to account for repeated measures.
413 Because variances were heterogenous for the photosynthesis data during the growth phase we used
414 a generalised linear mixed model including competition-specific variances. Finally, we integrated
415 photosynthesis and respiration rates over a 24-hour period to estimate net energy production of the
416 whole sample (J/day), as 14 hr of energy produced through net photosynthesis minus 10 hr of
417 respiration using rates predicted from the mixed models above.

418 We could not use mixed models on the oxygen evolution data from the first common garden because
419 of a singular fit error likely due to the lower replication of the interspecific competition treatment (n =
420 6). Therefore, we used linear models with biovolume (covariate) and competition treatment as
421 predictors (i.e. without including lineage identity). While this is not ideal, we repeated the analyses for
422 the second common garden with the same, simple linear models and obtained the same results of
423 mixed models (results not reported here), suggesting that oxygen rates are not strongly affected by
424 lineage identity. Nonetheless, we report the results on oxygen rates for the first common garden as a
425 supplementary figure. For all analyses of oxygen rates, data were not transformed but biovolume was
426 rescaled to 10^{-5} μm^3 μl^{-1}. Interactions between biovolume and competition were removed when $p >$
427 0.25 or if the interaction was not significant and the model with interaction did not perform better than
428 the simpler model compared by AIC and anova.

429 Demography. To test differences in the maximum rates of increase (r_{max}) and maximum values (K_{cells})
430 of cell density we followed a three-step approach (described in detail in Ghedini et al. [63], adapted from
431 Malerba et al. [71]). First, we fitted four growth models to each individual replicate lineage and chose the
432 best-fitting model among the four candidates to describe changes in the cell density (cells μl^{-1}) of
433 each culture over time. We used AIC to determine which growth model best described the dynamics
434 of a culture and successful convergence was ensured for all best-fitting models. The four models
435 were: a logistic-type sinusoidal growth model with lower asymptote forced to 0 (i.e. three-parameter
436 logistic curve), a logistic-type sinusoidal growth model with non-zero lower asymptote (i.e. four-
437 parameter logistic curve), a Gompertz-type sinusoidal growth model (i.e. three-parameter Gompertz
438 curve) and a modified Gompertz-type sinusoidal growth model including population decline after
439 reaching a maximum (i.e. four-parameter Gompertz-like curve including mortality). Second, we used
440 the best-fitting model to estimate growth parameters (i.e. r_{max} and K_{cells}) for each culture. From each

441 nonlinear curve, we extracted the maximum predicted value of population density (K_{cells}, cells μl^{-1}).
442 From the first derivative of the curve, we extracted the maximum rate of population increase (r_{max},
443 unit: day^{-1}). Third, we used an analysis of covariance to evaluate the influence of competition on each
444 parameter, using a linear model including the initial cell density estimated from the previous step as a
445 covariate and competition environment as a factor (three levels). The estimates of K_{cells} of the first
446 common garden had heterogeneous variances among treatments, so we used generalized least
447 squares models (instead of linear models) including treatment-specific variance for each level of
448 competition treatment (varIdent function in R). We then estimated and plotted least square means and
449 95% confidence intervals using Tukey p-value adjustment for comparing three estimates.

450 Scaling of demographic parameters with cell size. We determined the scaling of metabolism with cell
451 size for our evolved populations after ten weeks of evolution (~70 generation). For this assessment
452 we combined the data across the three competition treatments to assess a wider range of size. We
453 calculated the scaling of respiration and photosynthesis, separately, from linear models including cell
454 size and experiment day as numerical predictors. Oxygen rates and cell size were log_{10}-transformed.
455 Results did not qualitatively change when we analysed each competition treatment separately, as
456 each of them scaled > 1 and declined over time (Table S4).

457 Based on these results (effects of size and experiment day), we then calculated the expected scaling
458 of respiration with size for any given day. According to metabolic theory, the cost of production is
459 directly proportional to cell size (scales with size at 1) [17,25], so demographic parameters should scale
460 with size at:

461 (1) $r_{max} = M^{B}_{exponential}/M^{1} = M^{B-1}$
462 (2) $K_{cells} = M^{0}/M^{B}_{stationary} = M^{-B}$
463 (3) $K_{bio} = M \times K_{cells} = M \times M^{-B} = M^{1-B}$

464 We tested these predictions by comparing the predicted metabolic scaling values for the growth
465 phase and stationary phase to the observed metabolic scalings from our data. We used early (days 1-
466 5) respiratory scaling values for expectations about r_{max} because it is mostly determined by growth
467 rates early on ($B_{exponential}$ = 1.13). We used late (days 12-16) respiratory scaling values for
468 expectations about K_{cells} and K_{bio} ($B_{stationary}$ = 0.60) because cultures reached carrying capacity in the
469 latter part of the common garden and because cell size (which affects estimates of K_{bio}) stabilised

around day 12 (Fig. S2). We estimated maximum total biomass (K_{bio}) as the product of K_{cells} obtained from the population growth models and the average cell size for each replicate over the last three sampling days (day 12 to 16), when cell size stabilised. Finally, we determined the empirical scaling of each demographic parameter with cell size across the focal populations, using the average cell size calculated over the same intervals above (i.e., over the first 5 days for r_{max}, between day 12 and 16 for K_{cells} and K_{bio}).

Acknowledgements: We thank Mike McDonald and John DeLong for valuable comments on earlier versions of the manuscript. We also thank Jiaye Qin for assistance in data collection and the Quantitative Biology Unit at the Instituto Gulbenkian de Ciência for statistical advice. This work was supported by the Australian Research Council through a DECRA fellowship (DE190100660) and by a fellowship (LCF/BQ/PI21/11830001) from “la Caixa” Foundation (ID 100010434) and the European Union’s Horizon 2020 research and innovation programme under the Marie Skłodowska Curie grant agreement No 847648 to GG.

References

1. Aubree, F. *et al.* How community adaptation affects biodiversity–ecosystem functioning relationships. *Ecol. Lett.* **23**, 1263–1275 (2020).
2. Post, D. M. & Palkovacs, E. P. Eco-evolutionary feedbacks in community and ecosystem ecology: interactions between the ecological theatre and the evolutionary play. *Philos. Trans. R. Soc. B Biol. Sci.* (2009) doi:10.1098/rstb.2009.0012.
3. Hart, S. P., Turcotte, M. M. & Levine, J. M. Effects of rapid evolution on species coexistence. *Proc. Natl. Acad. Sci.* **116**, 2112 (2019).
4. Jousset, A., Eisenhauer, N., Merker, M., Mouquet, N. & Scheu, S. High functional diversity stimulates diversification in experimental microbial communities. *Sci. Adv.* **2**, e1600124 (2016).
5. Lawrence, D. *et al.* Species Interactions Alter Evolutionary Responses to a Novel Environment. *PLOS Biol.* **10**, e1001330 (2012).

6. Scheuerl, T. *et al.* Bacterial adaptation is constrained in complex communities. *Nat. Commun.* **11**, 754 (2020).
7. García, F. C. *et al.* The temperature dependence of microbial community respiration is amplified by changes in species interactions. *Nat. Microbiol.* **8**, 272–283 (2023).
8. Barraclough, T. G. How Do Species Interactions Affect Evolutionary Dynamics Across Whole Communities? *Annu. Rev. Ecol. Evol. Syst.* **46**, 25–48 (2015).
9. Grant, P. R. & Grant, B. R. Evolution of Character Displacement in Darwin's Finches. *Science* **313**, 224–226 (2006).
10. Rainey, P. B. & Travisano, M. Adaptive radiation in a heterogeneous environment. *Nature* **394**, 69–72 (1998).
11. Schluter, D. Experimental Evidence That Competition Promotes Divergence in Adaptive Radiation. *Science* **266**, 798–801 (1994).
12. Abrams, P. A. Alternative Models of Character Displacement and Niche Shift. I. Adaptive Shifts in Resource Use When There is Competition for Nutritionally Nonsubstitutable Resources. *Evolution* **41**, 651–661 (1987).
13. Fox, J. W. & Vasseur, D. A. Character Convergence under Competition for Nutritionally Essential Resources. *Am. Nat.* **172**, 667–680 (2008).
14. Gallego, I. & Narwani, A. Ecology and evolution of competitive trait variation in natural phytoplankton communities under selection. *Ecol. Lett.* **25**, 2397–2409 (2022).
15. TerHorst, C. P. *et al.* Evolution in a Community Context: Trait Responses to Multiple Species Interactions. *Am. Nat.* **191**, 368–380 (2018).
16. Brown, J. H., Gillooly, J. F., Allen, A. P., Savage, V. M. & West, G. B. Toward a metabolic theory of ecology. *Ecology* **85**, 1771–1789 (2004).
17. Savage, V. M., Gillooly, J. F., Brown, J. H., West, G. B. & Charnov, E. L. Effects of body size and temperature on population growth. *Am. Nat.* **163**, 429–441 (2004).
18. Damuth, J. Population-density and body size in mammals. *Nature* **290**, 699–700 (1981).
19. Isaac, N. J. B., Carbone, C. & McGill, B. Population and Community Ecology. in *Metabolic Ecology* (eds. Sibly, R. M., Brown, J. H. & Kodric-Brown, A.) (2012).
20. Malerba, M. E. & Marshall, D. J. Size-abundance rules? Evolution changes scaling relationships between size, metabolism and demography. *Ecol. Lett.* **22**, 1407–1416 (2019).

528 21. Berga, M., Székely, A. J. & Langenheder, S. Effects of disturbance intensity and frequency on
529 bacterial community composition and function. *PLoS ONE* **7**, e36959–e36959 (2012).
530 22. Pomati, F., Jokela, J., Castiglioni, S., Thomas, M. K. & Nizzetto, L. Water-borne pharmaceuticals
531 reduce phenotypic diversity and response capacity of natural phytoplankton communities. *PLoS*
532 *ONE* **12**, e0174207 (2017).
533 23. Poulson-Ellestad, K. L. *et al.* Metabolomics and proteomics reveal impacts of chemically
534 mediated competition on marine plankton. *Proc. Natl. Acad. Sci.* **111**, 9009 (2014).
535 24. de Villemereuil, P., Gaggiotti, O. E., Mouterde, M. & Till-Bottraud, I. Common garden experiments
536 in the genomic era: new perspectives and opportunities. *Heredity* **116**, 249–254 (2016).
537 25. Marshall, D. J. *et al.* Long-term experimental evolution decouples size and production costs in
538 Escherichia coli. *Proc. Natl. Acad. Sci.* **119**, e2200713119 (2022).
539 26. Bernhardt, J. R. *et al.* The evolution of competitive ability for essential resources. *Philos. Trans.*
540 *R. Soc. B Biol. Sci.* **375**, 20190247 (2020).
541 27. Bassar, R. D. *et al.* Experimental Evidence for Density-Dependent Regulation and Selection on
542 Trinidadian Guppy Life Histories. *Am. Nat.* **181**, 25–38 (2013).
543 28. Pianka, E. R. On r- and K-Selection. *Am. Nat.* **104**, 592–597 (1970).
544 29. Bierbaum, T. J., Mueller, L. D. & Ayala, F. J. Density-Dependent Evolution of Life-History Traits in
545 Drosophila Melanogaster. *Evolution* **43**, 382–392 (1989).
546 30. Mueller, L. D. & Ayala, F. J. Trade-off between r-selection and K-selection in Drosophila
547 populations. *Proc. Natl. Acad. Sci.* **78**, 1303–1305 (1981).
548 31. Gorter, F. A., Manhart, M. & Ackermann, M. Understanding the evolution of interspecies
549 interactions in microbial communities. *Philos. Trans. R. Soc. B Biol. Sci.* **375**, 20190256 (2020).
550 32. Falkowski, P. G., Fenchel, T. & Delong, E. F. The Microbial Engines That Drive Earth's
551 Biogeochemical Cycles. *Science* **320**, 1034–1039 (2008).
552 33. Field, C. B., Behrenfeld, M. J., Randerson, J. T. & Falkowski, P. Primary Production of the
553 Biosphere: Integrating Terrestrial and Oceanic Components. *Science* **281**, 237 (1998).
554 34. Hillebrand, H. *et al.* Cell size as driver and sentinel of phytoplankton community structure and
555 functioning. *Funct. Ecol.* **36**, 276–293 (2022).

35. Yvon-Durocher, G., Montoya, J. M., Trimmer, M. & Woodward, G. U. Y. Warming alters the size spectrum and shifts the distribution of biomass in freshwater ecosystems. *Glob. Change Biol.* **17**, 1681–1694 (2011).
36. Barton, S. *et al.* Evolutionary temperature compensation of carbon fixation in marine phytoplankton. *Ecol. Lett.* **23**, 722–733 (2020).
37. Padfield, D., Yvon-Durocher, G., Buckling, A., Jennings, S. & Yvon-Durocher, G. Rapid evolution of metabolic traits explains thermal adaptation in phytoplankton. *Ecol. Lett.* **19**, 133–142 (2016).
38. Govaert, L., Gilarranz, L. J. & Altermatt, F. Competition alters species' plastic and genetic response to environmental change. *Sci. Rep.* **11**, 23518 (2021).
39. Malerba, M. E., White, C. R. & Marshall, D. J. Eco-energetic consequences of evolutionary shifts in body size. *Ecol. Lett.* **21**, 54–62 (2017).
40. Bell, G. Experimental Evolution of Heterotrophy in a Green Alga. *Evolution* **67**, 468–476 (2013).
41. Collins, S. Competition limits adaptation and productivity in a photosynthetic alga at elevated CO2. *Proc Biol Sci* **278**, 247–55 (2011).
42. Maynard, D. S., Crowther, T. W. & Bradford, M. A. Competitive network determines the direction of the diversity–function relationship. *Proc. Natl. Acad. Sci.* **114**, 11464 (2017).
43. Vallina, S. M., Cermeno, P., Dutkiewicz, S., Loreau, M. & Montoya, J. M. Phytoplankton functional diversity increases ecosystem productivity and stability. *Ecol. Model.* **361**, 184–196 (2017).
44. Osmond, M. M. & de Mazancourt, C. How competition affects evolutionary rescue. *Philos Trans R Soc Lond B Biol Sci* **368**, 20120085–20120085 (2013).
45. MacArthur, R. H. & Wilson, E. O. *The Theory of Island Biogeography*. (Princeton University Press, 1967).
46. Sæther, B.-E., Visser, M. E., Grøtan, V. & Engen, S. Evidence for r- and K-selection in a wild bird population: a reciprocal link between ecology and evolution. *Proc. R. Soc. B Biol. Sci.* **283**, 20152411 (2016).
47. Lande, R., Engen, S. & Sæther, B.-E. An evolutionary maximum principle for density-dependent population dynamics in a fluctuating environment. *Philos. Trans. R. Soc. B Biol. Sci.* **364**, 1511–1518 (2009).

584 48. Kentie, R., Clegg, S. M., Tuljapurkar, S., Gaillard, J.-M. & Coulson, T. Life-history strategy varies
585 with the strength of competition in a food-limited ungulate population. *Ecol. Lett.* **23**, 811–820
586 (2020).
587 49. Gallego, I., Venail, P. & Ibelings, B. W. Size differences predict niche and relative fitness
588 differences between phytoplankton species but not their coexistence. *ISME J.* **13**, 1133–1143
589 (2019).
590 50. Brandl, S. J. *et al.* Metabolic rates mirror morphological and behavioral differences in two sand-
591 dwelling coral reef gobies. *Mar. Ecol. Prog. Ser.* **684**, 79–90 (2022).
592 51. Alexander, J. M., Diez, J. M. & Levine, J. M. Novel competitors shape species' responses to
593 climate change. *Nature* **525**, 515–518 (2015).
594 52. Lancaster, L. T., Morrison, G. & Fitt, R. N. Life history trade-offs, the intensity of competition, and
595 coexistence in novel and evolving communities under climate change. *Philos. Trans. R. Soc. B*
596 *Biol. Sci.* **372**, 20160046 (2017).
597 53. White, C. R., Alton, L. A., Bywater, C. L., Lombardi, E. J. & Marshall, D. J. Metabolic scaling is the
598 product of life-history optimization. *Science* **377**, 834–839 (2022).
599 54. Guillard, R. R. L. & Ryther, J. H. Studies of marine planktonic diatoms. I. *Cyclotella nana* Hustedt
600 and *Detonula confervacea* Cleve. *Can. J. Microbiol.* **8**, 229–239 (1962).
601 55. Schindelin, J. *et al.* Fiji: an open-source platform for biological-image analysis. *Nat. Methods* **9**,
602 676–682 (2012).
603 56. Hillebrand, H., Dürselen, C.-D., Kirschtel, D., Pollingher, U. & Zohary, T. Biovolume calculation for
604 pelagic and benthic microalgae. *J. Phycol.* **35**, 403–424 (1999).
605 57. Lenski, R. E. Phenotypic and Genomic Evolution during a 20,000-Generation Experiment with the
606 Bacterium Escherichia coli. in *Plant Breeding Reviews* 225–265 (John Wiley & Sons, Ltd, 2003).
607 doi:10.1002/9780470650288.ch8.
608 58. Grant, N. A., Abdel Magid, A., Franklin, J., Dufour, Y. & Lenski, R. E. Changes in Cell Size and
609 Shape during 50,000 Generations of Experimental Evolution with Escherichia coli. *J. Bacteriol.*
610 **203**, e00469-20 (2021).
611 59. Ryabov, A. *et al.* Shape matters: the relationship between cell geometry and diversity in
612 phytoplankton. *Ecol. Lett.* **24**, 847–861 (2021).

60. Litchman, E. & Klausmeier, C. A. Trait-Based Community Ecology of Phytoplankton. *Annu. Rev. Ecol. Evol. Syst.* **39**, 615–639 (2008).
61. Tan, H., Hirst, A. G., Atkinson, D. & Kratina, P. Body size and shape responses to warming and resource competition. *Funct. Ecol.* **35**, 1460–1469 (2021).
62. Malerba, M. E., White, C. R. & Marshall, D. J. Phytoplankton size-scaling of net-energy flux across light and biomass gradients. *Ecology* **98**, 3106–3115 (2017).
63. Ghedini, G., Marshall, D. J. & Loreau, M. Phytoplankton diversity affects biomass and energy production differently during community development. *Funct. Ecol.* **36**, 446–457 (2022).
64. Olito, C., White, C. R., Marshall, D. J. & Barneche, D. R. Estimating monotonic rates from biological data using local linear regression. *J. Exp. Biol.* **220**, 759 (2017).
65. White, C. R., Kearney, M. R., Matthews, P. G. D., Kooijman, S. A. L. M. & Marshall, D. J. A Manipulative Test of Competing Theories for Metabolic Scaling. *Am. Nat.* **178**, 746–754 (2011).
66. Williams, P. J. le B. & Laurens, L. M. L. Microalgae as biodiesel & biomass feedstocks: Review & analysis of the biochemistry, energetics & economics. *Energy Environ. Sci.* **3**, 554–590 (2010).
67. Pinheiro, J. & Bates, D. nlme: Linear and Nonlinear Mixed Effects Models. R package version 3.1-161. *R Core Team* (2022) doi:https://CRAN.R-project.org/package=nlme.
68. Bates, D., Mächler, M., Bolker, B. & Walker, S. Fitting Linear Mixed-Effects Models Using lme4. *2015* **67**, 48 (2015).
69. Fox, J. & Weisberg, S. An {R} Companion to Applied Regression, Third Edition. Thousand Oaks CA: Sage. URL: https://socialsciences.mcmaster.ca/jfox/Books/Companion/. (2019).
70. Wickham, H. ggplot2: Elegant Graphics for Data Analysis. *Springer-Verl. N. Y.* **ISBN 978-3-319-24277-4**, (2016).
71. Malerba, M. E., Palacios, M. M. & Marshall, D. J. Do larger individuals cope with resource fluctuations better? An artificial selection approach. *Proc. R. Soc. B Biol. Sci.* **285**, 20181347 (2018).